Superconductivity-induced re-entrance of the orthorhombic distortion in $Ba_{1-x}K_xFe_2As_2$

A.E. Böhmer[1,†], F. Hardy[1], L. Wang[1], T. Wolf[1], P. Schweiss[1] & C. Meingast[1]

Detailed knowledge of the phase diagram and the nature of the competing magnetic and superconducting phases is imperative for a deeper understanding of the physics of iron-based superconductivity. Magnetism in the iron-based superconductors is usually a stripe-type spin-density-wave, which breaks the tetragonal symmetry of the lattice, and is known to compete strongly with superconductivity. Recently, it was found that in some systems an additional spin-density-wave transition occurs, which restores this tetragonal symmetry, however, its interaction with superconductivity remains unclear. Here, using thermodynamic measurements on $Ba_{1-x}K_xFe_2As_2$ single crystals, we show that the spin-density-wave phase of tetragonal symmetry competes much stronger with superconductivity than the stripe-type spin-density-wave phase, which results in a novel re-entrance of the latter at or slightly below the superconducting transition.

Unconventional superconductivity often arises around the point where some kind of magnetic order (either antiferromagnetic or ferromagnetic) is suppressed by a tuning parameter, such as pressure or chemical substitution[1–3]. This led to the idea that superconducting pairing in these materials may result from the low-energy magnetic fluctuations surrounding the quantum critical point where magnetism is suppressed to zero temperature[4]. The magnetic ground state of typical iron-based superconducting parent compounds is a stripe-type antiferromagnetic spin-density wave (SDW) phase, which breaks the C_4 symmetry of the high-temperature tetragonal paramagnetic phase and is closely related to a tetragonal-to-orthorhombic structural distortion of the lattice[5]. An important debate, triggered by the observation that this orthorhombic structural distortion sometimes occurs slightly above the magnetic transition[6], concerns the respective roles of spin and orbital degrees of freedom[7,8]. In the orbital picture, the structural transition is due to orbital ordering and can trigger a, secondary, magnetic transition[8]. In the so-called spin-nematic scenario, on the other hand, magnetism is essential and the structural transition is really just the first step of the magnetic transition, induced by an Ising-nematic degree of freedom associated with the emerging stripe-type magnetic order[9]. Importantly, both orbital and spin fluctuations are candidates for the superconducting pairing[7,8].

A surprising recent result is the observation of a C_4-symmetric tetragonal magnetically ordered phase in $Ba_{1-x}Na_xFe_2As_2$ using neutron scattering[10], which was taken as evidence for the spin scenario because the existence of such a phase can hardly be reconciled with orbital order being a prerequisite for magnetism[10]. Up to now, a similar C_4-magnetic phase has not been observed in the closely related $Ba_{1-x}K_xFe_2As_2$ system, which was the first iron-based superconductor of 122-type stoichiometry to be discovered[11] and has the highest $T_c = 38$ K within this family. However, an unidentified phase transition in resistivity measurements under pressure[12] hints that an additional instability is close by. Earlier theoretical work indicates the close proximity in energy between C_4- and C_2-symmetric magnetic structures[13].

Here we re-examine the phase diagram of $Ba_{1-x}K_xFe_2As_2$ in unprecedented detail using thermal-expansion and specific-heat measurements of very high-quality single crystals. Within a narrow composition range, we observe a C_4-symmetric magnetic phase, which apparently has been missed in previous investigations[12,14–16]. In strong contrast to Na-doped $BaFe_2As_2$, the C_4-phase is, however, not stable to zero temperature and reverts back to the C_2 phase in the vicinity of the onset of superconductivity. This preference of superconductivity for the stripe-type C_2- over the C_4-magnetic state in this system may provide important clues about the superconducting pairing mechanism[17].

Results

Orthorhombic distortion. Figure 1 presents our first main result, the orthorhombic distortion $\delta = (a-b)/(a+b)$ (a and b are the in-plane lattice constants) versus temperature of underdoped $Ba_{1-x}K_xFe_2As_2$ obtained using our high-resolution capacitance dilatometer[18]. Even though dilatometry is a macroscopic probe, the thermal expansion of the individual a and b axes, as well as the distortion δ, can be derived using the difference between 'twinned' and 'detwinned' data sets, as shown previously for FeSe (ref. 19) and detailed in the supplementary material (Supplementary Figs 1 and 2). The reliability of this method, which has higher resolution by several orders of magnitude than either neutron or X-ray diffraction experiments, is demonstrated

by the close match to results of neutron powder diffraction[14] (see Fig. 1e). In $Ba_{1-x}K_xFe_2As_2$, the structural and magnetic transitions are coincident and first-order over the entire phase diagram[14]. Our curves in Fig. 1d, indeed, exhibit the well-known increase of δ at $T_{s,N}$ and the subsequent suppression of δ below T_c (ref. 20) for 22% K content. In the small concentration range $\sim$24.7–27.6% K content we find a surprising new result, namely, a sudden reduction of the orthorhombic distortion at $T_1 < T_{s,N}$, followed by a sudden increase at T_2 to a value slightly below its maximum value. This sudden reduction of δ strongly suggests that these $Ba_{1-x}K_xFe_2As_2$ samples undergo a similar transition to a C_4-magnetic phase as found in $Ba_{1-x}Na_xFe_2As_2$ (refs 10,21). The increase of δ at T_2, on the other hand, is an indication for re-entrance of the C_2-SDW phase. To prove that the intermediate phase is truly tetragonal, we have corrected the data of the 24.7% K crystal for the finite stress applied during the measurement, which induces non-zero distortion δ even in C_4-symmetric phases (Fig. 1f, see Supplementary Figs 1 and 2). The corrected value, δ_0, indeed vanishes completely (to within the extremely small value $\sim 0.01 \times 10^{-3}$, related to our error bar) in the intermediate phase, as expected for a truly tetragonal C_4 phase.

Similar to inverse melting[22], the counterintuitive transition at T_1 into a state of seemingly higher symmetry on lowering of the temperature does not violate the laws of thermodynamics. Rather, it convincingly demonstrates that the structural distortion is not the primary order parameter and that other degrees of freedom must be involved. The absolute measure for disorder is the entropy of the isolated system, which never increases with decreasing temperature. In the following we investigate the novel re-entrant transitions at T_1 and T_2 and their relation to superconductivity by examining the electronic entropy/heat capacity of the system. Moreover, the fact that δ below T_2 is still reduced from the value expected by extrapolation from the C_2-SDW phase (dashed black line for the 24.7% sample, red curve in Fig. 1d) suggests that the superconducting transition lies somewhere within the intermediate C_4 phase. Since no clear signature of superconductivity can be observed in the δ (T) curves, heat-capacity data are also crucial to nail down the location of the bulk superconducting transition.

Specific heat and electronic entropy. Figure 2 presents our electronic heat capacity C_e/T and electronic entropy divided by temperature $S_e/T = \frac{1}{T}\int C_e/T dT$, complemented by δ, and the temperature-dependent in-plane length change $\Delta L_{ab}/L_{ab}$ for 'twinned' samples (c axis data and thermal-expansion coefficients are given in the Supplementary Fig. 3) for various compositions. In a Fermi liquid, S_e/T is expected to be constant, and how the entropy is reduced on cooling through the transitions provides important information about the strength of the competing orders. For the 23.2% sample, the usual first-order tetragonal-to-orthorhombic transition occurs at $T_{s,N} = 81$ K and results in a sizable reduction of S_e/T. The remaining S_e/T is lost through superconductivity with an onset at $T_c = 24$ K (see Fig. 2a,f,k,p).

The lowest K concentration for which the C_4-magnetic phase is observed is 24.7% (Fig. 2b,g,l,q). Surprisingly, we do not observe a clear signature of a superconducting transition neither in C_e/T nor in L_{ab} for this crystal, while strong first-order peaks indicate $T_{s,N}$, T_1 and T_2 unambiguously. Nevertheless, the heat-capacity data show that the Fermi-surface is completely gapped at low temperature, implying a superconducting ground state. T_c is located by applying a large magnetic field. Notably, in a magnetic field of 12 T, the sharp peak at T_2 disappears and is replaced by a broadened step-like anomaly, which is slightly shifted downward in temperature from the peak at T_2, while the transitions at T_1
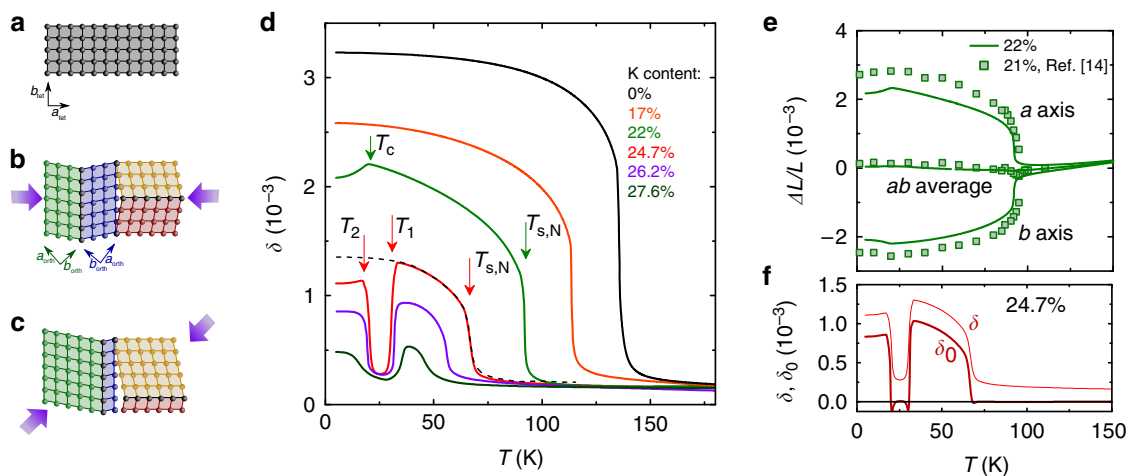
Figure 1 | Orthorhombic distortion of $Ba_{1-x}K_xFe_2As_2$ as measured using a capacitance dilatometer. (**a**) Schematic representation of the tetragonal C_4 high-temperature phase. (**b**) Representation of the structural domains formed in the orthorhombic C_2 phase ('twins', indicated by different colours). The domain structure is unaffected by the force from the spring-loaded dilatometer if it is applied along the tetragonal [100] in-plane direction (purple arrows). (**c**) Representation of the mostly 'detwinned' state, achieved by applying the dilatometer force along [110], which selects the domains with their (shorter) orthorhombic b axis along the direction of the applied force. (**d**) Temperature dependence of the orthorhombic distortion $\delta = (a-b)/(a+b)$ of underdoped $Ba_{1-x}K_xFe_2As_2$ obtained using difference of 'twinned' and 'detwinned' data from our high-resolution capacitance dilatometer. Abrupt changes of δ mark phase transitions, examples of which are indicated by vertical arrows. (**e**) Good agreement between our results (continuous lines), and results from neutron powder diffraction[14] (symbols) for the thermal expansion of the a and b axis demonstrates the reliability of our technique. (**f**) Orthorhombic distortion corrected for the effect of the applied force, δ_0, for the sample with 24.7% K content, distinguishing tetragonal and orthorhombic phases (see Supplementary Figs 1 and 2 for details on the measurement of the orthorhombic distortion).

and $T_{s,N}$ are hardly affected. The step-like anomaly, the shift and the broadening in field are expected for a superconducting transition, and we therefore identify this transition with T_c. This result implies that the strong specific-heat peak in zero-field at T_2 is a novel combined structural, magnetic and superconducting first-order transition, in which a re-entrance of the C_2-SDW phase occurs. How exactly a magnetic field tunes the system from a first- to second-order transition at T_c is a direction for future studies.

Increasing the K-content by just over 1% (to 26.2% K) drastically changes the behaviour. Superconductivity at $T_c = 26$ K can now easily be identified by the clear second-order specific-heat anomaly and a small kink in L_{ab} (Fig. 2h,m). The specific-heat anomaly is again broadened and shifted to lower temperatures by a high magnetic field. Superconductivity now coexists with the intermediate C_4 phase and reentrance of the C_2 phase occurs at $T_2 < T_c$, as evidenced by the increase of δ and L_{ab} (Fig. 2c,h). Surprisingly, there is only a very small anomaly in the heat capacity at T_2 (Fig. 2m). At still a slightly higher K content (27.6% K, Fig. 2d,i,n,s), no more anomaly that could be associated with T_2 is observed in either the heat capacity or in L_{ab}. The weak re-emergence of the orthorhombic distortion at low temperature is likely induced by the stress applied for detwinning. For this sample, the reduction of S_e/T is mainly due to superconductivity, and the magnetic and structural phase transitions at $T_{s,N}$ and T_1 play only a very minor role. Finally, Fig. 2e,j,o,t show the results for a sample with 30% K content, which undergoes only a superconducting transition. Note the larger specific-heat anomaly, which implies a considerably larger superconducting condensation energy than for the other samples.

Our heat-capacity data also show a striking low-temperature contribution to the electronic specific heat, or equivalently to the entropy, in the superconducting state for samples with 26.2 and 27.6% K content (see Fig. 2m,n,r,s). This feature, which is very reminiscent of the very small superconducting gaps found in KFe_2As_2 (ref. 23), is a sign of excited quasiparticles far below T_c and seems to occur only when the structural-magnetic transitions

are weak, that is, induce only a small entropy change. From the position of the maximum in C_e/T, we estimate for the size of the smallest superconducting gap $\Delta_{SC} \sim 0.07k_BT_c$ in the multigap system, which is even smaller than the 'lilliputian' gaps in KFe_2As_2 (ref. 23). The occurrence of such an extremely small gap may be related to peculiar features of the Fermi surface resulting from a reconstruction at $T_{s,N}$ and T_1 (see below). When this reconstruction becomes weaker on K doping, some parts of the reconstructed Fermi surface may move to within the superconducting gap Δ_{SC} of the Fermi level and can contribute to the superconducting condensate, as recently argued by Koshelev et al.[24]. This would explain why this low-temperature feature suddenly disappears once $T_{s,N}$ and T_1 are suppressed by doping (see Fig. 2o,t).

Phase diagram. The transition temperatures from Fig. 2 are summarized in the phase diagram of Fig. 3a together with additional thermodynamic data covering the whole phase diagram[25], (F. Hardy et al., manuscript in preparation). We find five distinct thermodynamic ordered phases, which all compete for the electronic entropy provided by the high-temperature C_4-paramagnetic phase: C_2 SDW, C_4 magnetic, C_2 SDW coexisting with superconductivity, C_4 magnetic coexisting with superconductivity and C_4-superconducting. Strikingly, T_c drops by about 7 K on going from the C_2- to the C_4-magnetic phase and, similarly, T_c increases by about 6 K at the boundary from the C_4-magnetic to the C_4-paramagnetic state. This points to a much stronger competition between superconductivity and the C_4-magnetic phase than between superconductivity and the C_2-magnetic phase, which is probably due to the additional pronounced suppression of entropy at T_1 (see Fig. 2q). In particular, it would be clearly thermodynamically advantageous for superconductivity if the system would revert back to the C_2-magnetic phase with the higher electronic entropy available for superconducting pairing. The system apparently does just this via a peculiar first-order magnetic, structural and
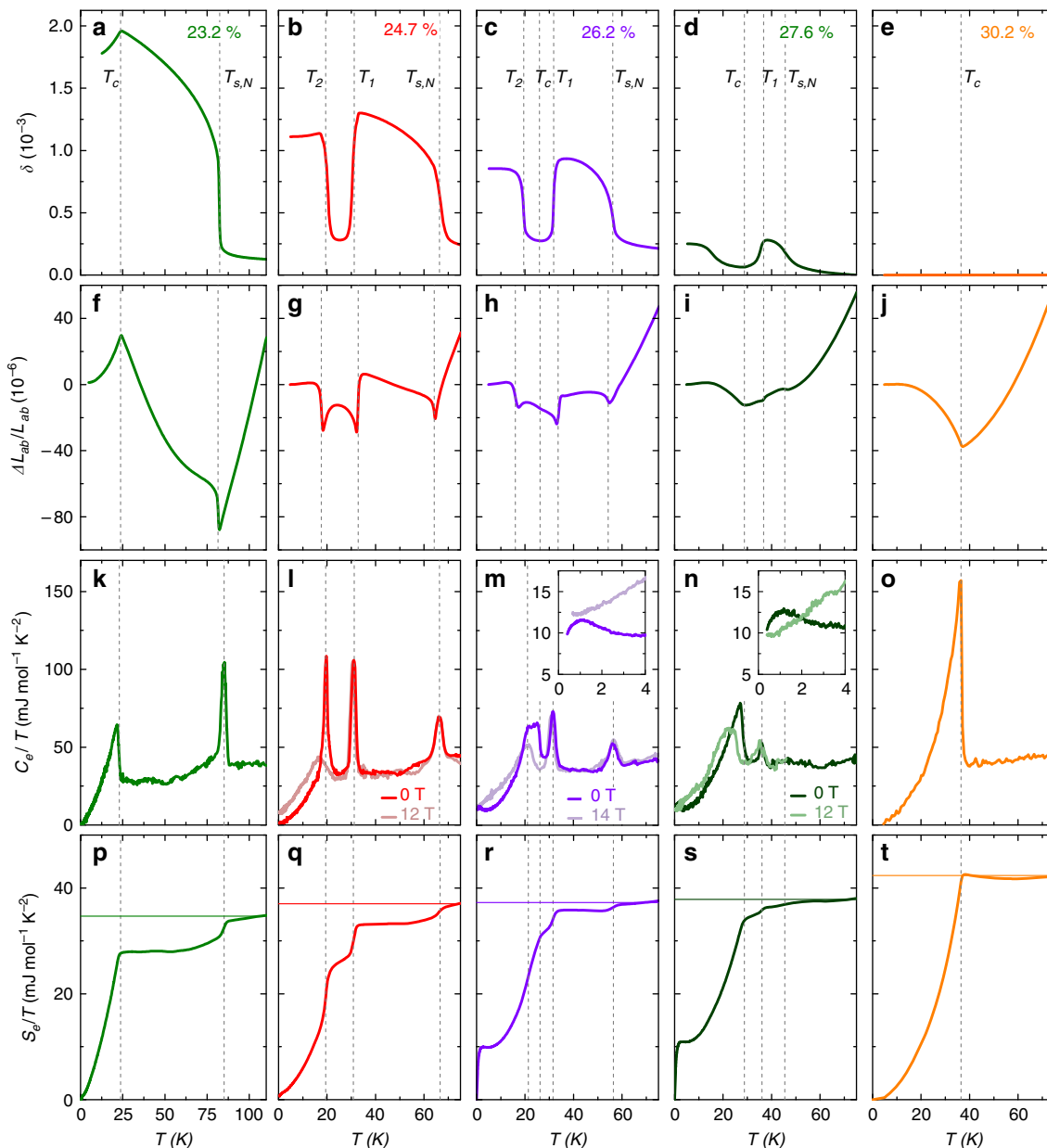
Figure 2 | Phase transitions in thermal expansion and electronic specific heat for 5 samples of different K content. (**a**–**e**) Orthorhombic distortion δ, (**f**–**j**) average in-plane length change $\Delta L_{ab}/L_{ab}$ for 'twinned' samples (**k**–**o**) electronic specific heat C_e/T, (**p**–**t**) electronic entropy divided by temperature S_e/T. Horizontal lines indicate the value of S_e/T of the high-temperature paramagnetic phase which is lost on cooling through the various transitions. (**l**–**n**) also show data measured in a large magnetic field and the insets show a magnification of the low-temperature region. Vertical lines mark the transitions temperatures labelled in panels (**a**–**e**).

superconducting transition at T_2 for the crystal with 24.7% K content. On further K doping, T_1 increases slightly, even though the entropy reduction at T_1 becomes significantly weaker. Apparently, this renders the coexistence of superconductivity and the C_4-magnetic phase possible, diminishing the driving force of the re-entrant transition at T_2.

The interplay between different thermodynamic phases is also reflected in the effect of pressure on the phase diagram. We infer the effect of uniaxial, in-plane average, pressure p_{ab} on the phase diagram from our thermal-expansion and specific-heat data using thermodynamic relations (see Methods) and the results are shown in Fig. 3b. For example, when superconductivity coexists with the C_2-SDW phase the uniaxial-pressure dependences $dT_{s,N}/dp_{ab} < 0$ and $dT_c/dp_{ab} > 0$ are of opposite sign and rather large showing the well-known competition of these two phases.

Interestingly, a similar competition between the two magnetic phases is implied by the derivatives $dT_{s,N}/dp_{ab} < 0$ and $dT_1/dp_{ab} > 0$. However, $dT_c/dp_{ab} \approx -1$ K GPa^{-1} is relatively small within the C_4 magnetic phase, even though T_1 and T_2 are very sensitive to p_{ab}. Note that the strong competition between superconductivity and the C_2-SDW phase manifests itself by a strong coupling of both order parameters to the orthorhombic distortion, and clearly such a coupling is not possible in a tetragonal state, which might explain this small value. Finally, it is interesting that, within the whole range from 28 to 100% K content, the T_c line is very smooth and $dT_c/dp_{ab} \approx -(2-3)$ K GPa^{-1} changes only weakly with doping. This suggests that the superconducting state does not change over the whole phase diagram and, in particular, does not undergo a symmetry change[26].
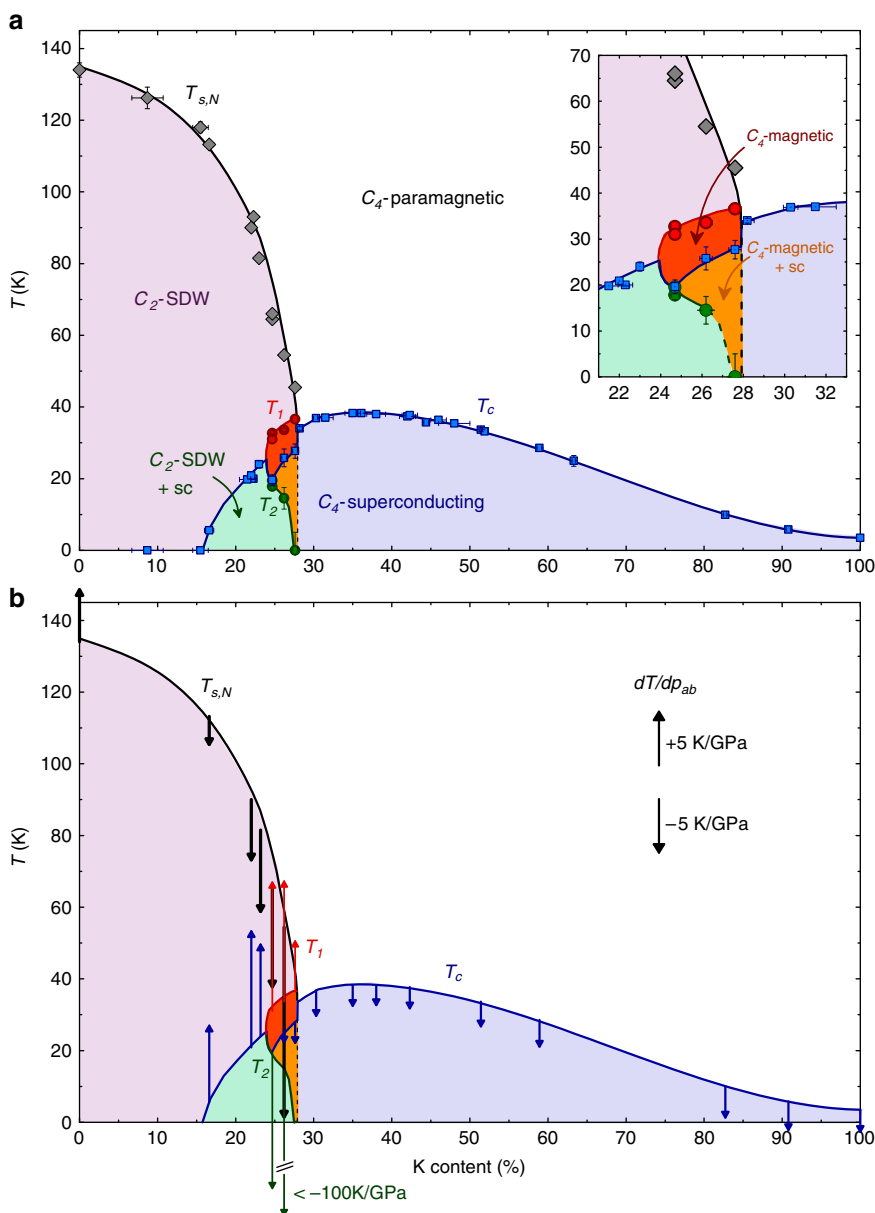
Figure 3 | Detailed phase diagram of $Ba_{1-x}K_xFe_2As_2$. (**a**) Phase diagram of $Ba_{1-x}K_xFe_2As_2$ spanning the whole substition range. $T_{s,N}$, T_1, T_2 and T_c (determined from the data shown in Fig. 2 and additional thermodynamic data) are shown by symbols. Lines and coloured areas are a guide to the eye indicating the five distinct thermodynamically ordered phases. A narrow region of a C_4-symmetric (tetragonal) magnetic phase, occurring within the usual C_2-symmetric (orthorhombic) SDW phase, is observed. It coexists with superconductivity with a reduced T_c. Superconductivity-induced reentrance of the C_2-SDW phase occurs at T_2. The inset shows an enlarged view of the region containing the C_4-magnetic phase. Vertical error bars indicate the uncertainty in the transition temperatures and horizontal error bars indicate the statistical error in the sample composition. (**b**) Predicted effect of uniaxial in-plane pressure p_{ab} on the phase diagram, from thermodynamic relations using our thermal-expansion and heat-capacity data. The direction of the arrows indicates the sign of the pressure derivative of the transition temperature and the length is proportional to its absolute value (see scale). Lines are reproduced from panel (**a**).

Discussion

The C_4 state which we observe in K-doped $BaFe_2As_2$ is very reminiscent of the magnetic C_4 phase observed in Na-doped $BaFe_2As_2$ (ref. 10), and is also probably closely related to the pressure-induced phase found in $Ba_{1-x}K_xFe_2As_2$ (ref. 12) (see Supplementary Fig. 4). This suggests that the occurrence of the C_4 phase is a universal property of the hole-doped 122-materials, which are expected to be 'cleaner' than the electron-doped ones. The most striking difference to $Ba_{1-x}Na_xFe_2As_2$ is the sudden re-emergence of δ, that is, the re-entrance of the C_2-SDW phase, below $T_2 \leq T_c$ in $Ba_{1-x}K_xFe_2As_2$. One explanation for this difference may be the lower stability of the C_4 phase, indicated

by considerably lower values of T_1. It is possibly related to a chemical pressure effect, since our results show that the magnetic C_4 phase in $Ba_{1-x}K_xFe_2As_2$ is extremely sensitive to (uniaxial) pressure (Fig. 3b). In particular, in-plane pressure is expected to strongly increase the extent of the C_4-magnetic phase, similar to hydrostatic pressure[12].

Several authors[10,17,27–30] have suggested that the detailed nature of the additional magnetic phase can hold important clues regarding the spin-orbital debate. As pointed out in ref. 10, the existence of a C_4-symmetric magnetic phase shows that the orthorhombic distortion is not necessary for magnetism which strongly supports the spin-nematic scenario. Concerning the

magnetic structure, such a phase is possible when there are two antiferromagnetic propagation vectors and the iron magnetic moments are either non-collinear or non-uniform[13,27,31]. On the other hand, magnetic neutron scattering results on $Ba_{1-x}Na_xFe_2As_2$ single crystals point to a re-orientation of the magnetic moments from in-plane to c axis orientated as the main element of the transition at T_1 and call for further study on whether the magnetic structure really has C_4 symmetry. Incidentally, the observed spin-re-orientation demonstrates that spin-orbit coupling cannot be neglected, and more theoretical work explicitly including this coupling is needed. Using the specific heat data, we can address the nature of these phase transitions from a thermodynamic point of view. In particular, the large entropy jump at the T_1 transition is not expected for a simple spin reorientation. Rather, our data imply that a significant change of the band structure occurs, which may be more in line with the emergence of a second SDW order parameter in the itinerant spin-nematic viewpoint[12,17]. Moreover, our high-resolution data demonstrate that the orthorhombic distortion vanishes in the second magnetic phase with an error bar of less than 1% of its maximum value, which strongly suggests that the phase is truly C_4-symmetric and that spin re-orientation is not the only element of the transition. Our data also show that superconductivity has a significant impact and can tip the balance between the two magnetic states in favour of the C_2-symmetric one. Very recent theoretical works based on three-band itinerant fermionic or five-band tight-binding approaches in fact find surprisingly good qualitative agreement with our experimental phase diagram, suggesting that the physics of the hole-doped materials can be understood fairly well within these frameworks[17,30]. In particular, the suppression of superconductivity within the C_4 phase and the re-entrance back into the C_2 phase is captured in the work of ref. 30.

In summary, a new and very detailed phase diagram of $Ba_{1-x}K_xFe_2As_2$, revealing intriguing new interactions between superconductivity and magnetism, has been derived from thermodynamic measurements. In particular, we find evidence for a narrow region of a C_4-symmetric magnetic phase which competes more strongly with superconductivity than the C_2-symmetric SDW phase. This competition between the two magnetic phases and superconductivity for the electronic entropy of the system results in a novel re-entrance of the C_2-symmetric phase either as a magneto-structural transition within the superconducting phase or as a peculiar first-order concomitant superconducting, structural and magnetic transition, both of which are exceptional for strongly correlated systems. The strong reduction of entropy associated with the second magnetic phase suggests it to be a C_4-type SDW in an itinerant scenario, rather than a simple spin re-orientation transition, in good agreement with recent theoretical work[17,30]. There are, however, still some unresolved issues, including the exact magnetic structure and the role of orbitals in this C_4 SDW phase. The existence of the C_4 phase at ambient pressure in high-quality single crystals opens up the possibility for studies using a large variety of more microscopic probes, such as magnetic neutron scattering, nuclear magnetic resonance, and angle-resolved photoemission studies, which will hopefully unravel some of these mysteries. Finally, we note that our preliminary thermodynamic studies on the $Ba_{1-x}Na_xFe_2As_2$ system show that this system is even more complicated than thought at present[10], and a detailed comparison between the K- and Na-doped systems will be very useful (L. Wang et al., manuscript in preparation).

Methods

Sample preparation and characterization. High-quality $Ba_{1-x}K_xFe_2As_2$ samples were grown by a self-flux technique in alumina crucibles sealed in iron cylinders using very slow cooling rates of 0.2–0.4 °C per h. They were *in situ* annealed by further slow cooling to room temperature. Single crystals with a mass of 1–3 mg were chosen for measurement and the composition of the five main samples of this article was determined by refinement of four-circle single-crystal X-ray diffraction patterns of a small piece of each crystal to be $x = 0.232(3)$, 0.247(2), 0.262(3), 0.276(2), 0.302(35). Good homogeneity is attested by the sharp thermodynamic transitions. The phase diagram in Fig. 3 is compiled using thermodynamic measurements of samples whose K content was determined by either single-crystal X-ray diffraction refinement or energy dispersive X-ray spectroscopy.

Thermal-expansion and specific-heat measurements. Uniaxial thermal expansion was measured in a home-made capacitance dilatometer[18] and specific heat in a Physical Property Measurement System from Quantum Design. The electronic specific heat was obtained by subtracting (F. Hardy et al., manuscript in preparation), from the raw data, a concentration-weighted sum of the lattice heat capacity of KFe_2As_2 and $Ba(Fe_{0.85}Co_{0.15})_2As_2$ derived from refs 23 and 32.

Determination of uniaxial pressure derivatives. Uniaxial-pressure derivatives were obtained from the Clausius–Clapeyron relation $dT/dp_{ab} = V_m(\Delta L_{ab}/L_{ab})/\Delta S$ for first-order phase transitions ($T_{s,N}$, T_1 and T_2) and from the Ehrenfest relation, $dT/dp_{ab} = V_m\Delta\alpha_{ab}/\Delta(C/T)$ for second-order phase transitions (T_c). Here, p_{ab} is the average in-plane pressure, $\alpha_{ab} = 1/L_{ab}dL_{ab}/dT$ the thermal expansion coefficient and ΔL_{ab}, ΔS and $\Delta\alpha_{ab}$ are the discontinuities at the phase transition and $V_m = 61.4\,cm^3\,mol^{-1}$ is the molar volume, which hardly changes on K substitution.

References

1. Flouquet, J. On the heavy fermion road. *Prog. Low Temp. Phys.* **15,** 139–281 (2005).
2. Pfleiderer, C. Superconducting phases of *f*-electron compounds. *Rev. Mod. Phys.* **81,** 1551–1624 (2009).
3. Norman, M. R. The challenge of unconventional superconductivity. *Science* **332,** 169 (2011).
4. Marthur, N. D. *et al.* Magnetically mediated superconductivity in heavy fermion compounds. *Nature* **394,** 39–43 (1998).
5. Paglione, J. & Greene, R. L. High-temperature superconductivity in iron-based materials. *Nat. Phys.* **6,** 645–658 (2010).
6. Canfield, P. C. & Bud'ko, S. L. FeAs-based superconductivity: a case study of the effects of transition metal doping on $BaFe_2As_2$. *Annu. Rev. Condens. Matter Phys.* **1,** 27–50 (2010).
7. Fernandes, R. M., Chubukov, A. V. & Schmalian, J. What drives nematic order in iron-based superconductors? *Nat Phys* **10,** 97–104 (2014).
8. Kontani, H., Saito, T. & Onari, S. Origin of orthorhombic transition, magnetic transition, and shear-modulus softening in iron pnictide superconductors: Analysis based on the orbital fluctuations theory. *Phys. Rev. B* **84,** 024528 (2011).
9. Fernandes, R. M. & Schmalian, J. Manifestations of nematic degrees of freedom in the magnetic, elastic, and superconducting properties of the iron pnictides. *Supercond. Sci. Technol.* **25,** 084005 (2012).
10. Avci, S. *et al.* Magnetically driven suppression of nematic order in an iron-based superconductor. *Nat. Commun.* **5,** 3845 (2014).
11. Rotter, M., Tegel, M. & Johrendt, D. Superconductivity at 38 K in the iron arsenide $Ba_{1-x}K_xFe_2As_2$. *Phys. Rev. Lett.* **101,** 107006 (2008).
12. Hassinger, E. *et al.* Pressure-induced Fermi-surface reconstruction in the iron-arsenide superconductor $Ba_{1-x}K_xFe_2As_2$: Evidence of a phase transition inside the antiferromagnetic phase. *Phys. Rev. B* **86,** 140502 (2012).
13. Lorenzana, J., Seibold, G., Ortix, C. & Grilli, M. Competing orders in FeAs layers. *Phys. Rev. Lett.* **101,** 186402 (2008).
14. Avci, S. *et al.* Magnetoelastic coupling in the phase diagram of $Ba_{1-x}K_xFe_2As_2$ as seen via neutron diffraction. *Phys. Rev. B* **83,** 172503 (2011).
15. Avci, S. *et al.* Phase diagram of $Ba_{1-x}K_xFe_2As_2$. *Phys. Rev. B* **85,** 184507 (2012).
16. Tanatar, M. A. *et al.* Interplane resistivity of underdoped single crystals $(Ba_{1-x}K_x)Fe_2As_2$ ($0 \leq x \leq 0.34$). *Phys. Rev. B* **89,** 144514 (2014).
17. Kang, J., Wang, X., Chubukov, A. V. & Fernandes, R. M. Interplay between tetragonal magnetic order, stripe magnetism, and superconductivity in iron-based materials. *Phys. Rev. B* **91,** 121104 (2015).
18. Meingast, C. *et al.* Anisotropic pressure dependence of T_c in single crystal $YBa_2Cu_3O_7$ via thermal expansion. *Phys. Rev. B* **41,** 11299–11304 (1990).
19. Böhmer, A. E. *et al.* Lack of coupling between superconductivity and orthorhombic distortion in stoichiometric single-crystalline FeSe. *Phys. Rev. B* **87,** 180505 (2013).
20. Wiesenmayer, E. *et al.* Microscopic coexistence of superconductivity and magnetism in $Ba_{1-x}K_xFe_2As_2$. *Phys. Rev. Lett.* **107,** 237001 (2011).
21. Waßer, F. *et al.* Spin reorientation in $Ba_{0.65}Na_{0.35}Fe_2As_2$ studied by single-crystal neutron diffraction. *Phys. Rev. B* **91,** 060505 (2015).
22. Greer, A. L. Too hot to melt. *Nature* **404,** 134–135 (2000).
23. Hardy, F. *et al.* Multiband superconductivity in KFe_2As_2: Evidence for one isotropic and several lilliputian energy gaps. *J. Phys. Soc. Jpn.* **83,** 014711 (2014).

24. Koshelev, A. E. & Matveev, K. A. Anomalous density of states in multiband superconductors near the Lifshitz transition. *Phys. Rev. B* **90,** 140505 (2014).

25. Böhmer, A. E. *Competing Phases in Iron-Based Superconductors Studied by High-Resolution Thermal-Expansion and Shear-Modulus Measurements.* Ph.D. thesis, Fakultät für Physik, Karlsruhe Institute of Technology (2014).

26. Fernandes, R. M. & Millis, A. J. Nematicity as a probe of superconducting pairing in iron-based superconductors. *Phys. Rev. Lett.* **111,** 127001 (2013).

27. Khalyavin, D. D. *et al.* Symmetry of reentrant tetragonal phase in $Ba_{1-x}Na_xFe_2As_2$: Magnetic versus orbital ordering mechanism. *Phys. Rev. B* **90,** 174511 (2014).

28. Wang, X. & Fernandes, R. M. Impact of local-moment fluctuations on the magnetic degeneracy of iron arsenide superconductors. *Phys. Rev. B* **89,** 144502 (2014).

29. Wang, X., Kang, J. & Fernandes, R. M. Magnetic order without tetragonal-symmetry-breaking in iron arsenides: Microscopic mechanism and spin-wave spectrum. *Phys. Rev. B* **91,** 024401 (2015).

30. Gastiasoro, M. N. & Andersen, B. M. Competing magnetic double-Q phases and superconductivity-induced re-entrance of C_2 magnetic stripe order in iron pnictides. Preprint at http://arxiv.org/abs/1502.05859 (2015).

31. Giovannetti, G. *et al.* Proximity of iron pnictide superconductors to a quantum tricritical point. *Nat. Commun.* **2,** 398 (2011).

32. Hardy, F. *et al.* Calorimetric evidence of multiband superconductivity in $Ba(Fe_{0.925}Co_{0.075})_2As_2$ single crystals. *Phys. Rev. B* **81,** 060501 (2010).

Additional information

Supplementary Information accompanies this paper at http://www.nature.com/naturecommunications

Competing financial interests: The authors declare no competing financial interests.

Reprints and permission information is available online at http://npg.nature.com/reprintsandpermissions/

How to cite this article: Böhmer, A.E. *et al.* Superconductivity-induced reentrance of the orthorhombic distortion in $Ba_{1-x}K_xFe_2As_2$. *Nat. Commun.* 6:7911 doi: 10.1038/ncomms8911 (2015).